

Temperature-Dependent Thévenin Model of a Li-Ion Battery for Automotive Management and Control

*Original*

Temperature-Dependent Thévenin Model of a Li-Ion Battery for Automotive Management and Control / Rizzello, A.; Scavuzzo, S.; Ferraris, A.; Airale, A. G.; Carello, M.. - ELETTRONICO. - (2020), pp. 1-6. ( 2020 IEEE International Conference on Environment and Electrical Engineering and 2020 IEEE Industrial and Commercial Power Systems Europe, IEEEIC / I and CPS Europe 2020 esp 2020) [10.1109/IEEEIC/ICPSEurope49358.2020.9160544].

*Availability:*

This version is available at: 11583/2910434 since: 2021-07-01T11:03:14Z

*Publisher:*

Institute of Electrical and Electronics Engineers Inc.

*Published*

DOI:10.1109/IEEEIC/ICPSEurope49358.2020.9160544

*Terms of use:*

This article is made available under terms and conditions as specified in the corresponding bibliographic description in the repository

*Publisher copyright*

(Article begins on next page)

# Temperature-Dependent Thévenin Model of a Li-Ion Battery for Automotive Management and Control

Alessandro Rizzello  
DIMEAS  
*Politecnico di Torino*  
Torino, Italy  
alessandro.rizzello@polito.it

Andrea Giancarlo Airale  
DIMEAS  
*Politecnico di Torino*  
Torino, Italy  
andrea.airale@polito.it

Santo Scavuzzo  
DIMEAS  
*Politecnico di Torino*  
Torino, Italy  
santo.scavuzzo@polito.it

Massimiliana Carello  
DIMEAS  
*Politecnico di Torino*  
Torino, Italy  
massimiliana.carello@polito.it

Alessandro Ferraris  
DIMEAS  
*Politecnico di Torino*  
Torino, Italy  
alessandro.ferraris@polito.it

## **Abstract**

This paper focuses on the analysis of Li-ion battery behavior at different temperatures through the Thévenin electrical circuit model. First, evaluations for both steady-state and dynamic battery applications are provided, then an overview of the different battery models to describe their dynamic behavior is analyzed. The focus is dedicated to the double polarization Thévenin-based equivalent circuit model since it represents an optimal trade-off between accuracy and computation effort, which justifies its implementation in a Battery Management System (BMS) for automotive real-time monitoring and control. The model is composed of a voltage source, one series resistor and two series RC blocks. The Hybrid Pulse Power Characterization test (HPPC) is performed inside a climatic chamber to extract the electrical parameters of the model and their dependency from both temperature and State Of Charge (SOC). The load-current effects on the battery performance are not considered for the simplicity and lightness of the presented model. The presented procedure has broader validity and is mostly independent of cell format and Li-ion chemistry, despite a specific cylindrical battery cell is chosen for the study. The results of the test are suitable for the future implementation of a proper algorithm for SOC and State Of Health SOH estimations. Moreover, they provide an effective electrical and thermal characterization of the cell to evaluate the heat generation rate inside the cell.

## **Keywords**

*lithium-ion battery, battery model, Electrical Equivalent Circuit (EEC), Dual-Polarization (DP), electric vehicles, temperature analysis, automotive applications, control.*

## **I. INTRODUCTION**

In the last few years, renewable energy sources have caught on in the global market due to an increasing awareness of the modern society about environmental issues, such as global warming, CO<sub>2</sub> emission, and dependency on fossil fuels. However, renewable technologies have an intermittent nature, thus they must be coupled with an effective energy storage system to enhance their performances and make them competitive with other energy production systems. Furthermore, hybrid and Electric Vehicles (EVs) represent a promising solution to reduce environmental pollution. Among Battery Electrochemical Energy Storage (BEES), Li-Ion Batteries (LIBs) are considered the best solution due to their high energy-to-weight ratio, lack of memory effect, fast response, high power capability, long-cycle lifetime at partial cycles, low self-discharge rates, and decreasing manufacturing costs [1].

The state of the art, future perspectives and most suitable applications according to different Li-ion chemistries are shown in [2], [3]. Lithium-Nickel-Manganese-Cobalt oxide (NMC) batteries show good specific energy, high power density, and good durability, these properties make them suitable for automotive application where strong dynamic profiles are involved [2]. Generally, electric vehicles can be classified in Hybrid Electric Vehicles (HEVs), Plugin Hybrid Electric Vehicles (PHEVs), Battery-powered Electric Vehicles (BEVs) and Fuel Cell Vehicles (FCVs) according to the power source [4], [5].

Although the Li-ion batteries represent the most suitable solution for energy storage due to their high performances, one of the major limitations to their complete diffusion in the market is the key-role of the operating temperature. Generally, the acceptable temperature range for LIBs is -20 °C ~ 60 °C [6], however, the optimal temperature region is 15°C – 35°C [7]. Working outside this range leads to the fast degradation of the cell with a high risk of safety problems such as fire and explosion. At low operation temperature, a reduction of chemical-reaction activity and charge-transfer velocity [6] occurs, which means a lower ionic conductivity in the electrolyte [8] and a reduction of lithium-ion diffusivity in the electrodes [9]. These microscopic phenomena lead to a reduction of energy and power capability at a macroscopic level. High-temperature operation is caused by steep internal temperature due to the large discharge/charge current rather than high environmental temperature. Even in these conditions, a decrease in capacity and power occurs. In extreme situations, where the temperature cannot be controlled anymore, a thermal runaway occurs which can lead to a self-ignition and explosion [10]. Therefore, a thermal management system is required to make the battery operate within a permitted temperature range and at the same time to avoid large temperature differences throughout the overall system [11].

Li-ion battery performances are affected by operation conditions, thus a Battery Management System (BMS) is crucial to monitor and control energy flows inside all EV subsystems, such as charging and discharging control, battery cell voltage monitoring, battery balancing, and charge equalization, input/output current and voltage monitoring, temperature control, battery safety and so on. Measurements and controls are performed by the BMS to estimate the State Of Charge (SOC) and the State Of Health (SOH) of the battery cells, to guarantee safe battery operation avoiding cell undervoltage, overvoltage, undertemperature, overtemperature and overcurrent [3], [12]. The BMS maximizes the life and performances of the battery.

The automotive sector is characterized by an extremely dynamic load profile in which high performances, reliability and safety are required. Therefore, optimal design, diagnosis and operation are demanded at both cell and system levels. Li-ion batteries have complex behavior characterized not only by chemical composition and materials involved in electrodes and electrolytes but it's also a function of a great number of variables such as temperature, state of charge, state of health and aging. Moreover, all these variables are linked together to form a high non-linear system with no internal measurable

properties. Only some quantities can be directly measured such as external temperature, voltage and current. Thus, battery models are necessary to provide insight into the battery and to guarantee optimal design and operation also when temporal changes of state variables occur [13].

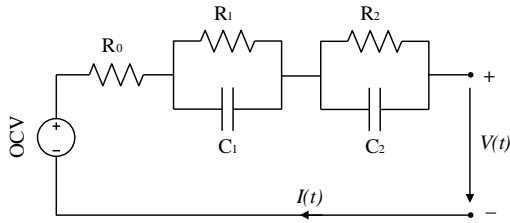


Fig. 1 2<sup>nd</sup> order Thévenin control circuit model

Literature provides a lot of battery models, typically they are classified in: physical, data-driven and equivalent circuit models. Accuracy, complexity and physical interpretability of the model are the parameters generally used to compare the afore-mentioned categories. The accuracy is an indicator of the quality of the estimated battery parameters, the complexity is linked to the computational time required to solve the model and it is a function of the number of variables involved in the model. This parameter is useful to indicate if a model is suitable for real-time applications. Finally, the physical interpretability states if the model provides an accurate explanation of the physics inside the battery [14].

Physical models are based on conservation principles and differential equations with which can describe the internal structure of the battery from a thermodynamic, kinetic and transport phenomena point of view. Analyzing a great number of parameters, they provide high accuracy and physical interpretability, although a considerable computational effort is required. On the contrary, data-driven models are made of empirical parameters and measured data without any physical interpretability. They require small computation time, but their accuracy is limited too. Finally, equivalent circuit models represent a suitable trade-off between physical and empirical models.

The idea of the models presented in this paper is to replace complex electrochemical processes with simple electric circuit components such as resistors and capacitors. They are characterized by enough accuracy and poor computational effort. Equivalent Electric Circuit models (EEC) are split into two categories: Impedance-based models and Thévenin-based models [14].

Impedance-based models [15] apply Electrochemical Impedance Spectroscopy (EIS) test to measure the impedance value of electrochemical systems [16], [17]. The impedance measurement consists of the dynamic voltage response measurement after a small alternating current supply [18]. Due to the presence of non-linear components, particular instrument required and complexity to extract model parameters, impedance-based models are out of the scope of this paper. On the contrary, Thévenin-based models are suitable for automotive applications thanks to their simplicity in terms of both parameterization and computational efforts, which justifies the feasibility of these models in BMS for real-time application.

This paper aims to evaluate experimentally the dependence of Thevenin electrical circuit parameters from both state of charge and temperature to implement a suitable algorithm for realistic SOC and SOH estimations. Moreover, a proper experimental characterization of the cells is useful to evaluate the heat generation rate during a charge/discharge current profile of the battery. The results of the test can be further used as input for a battery thermal model to investigate the evolution of temperature distribution inside the cell and design a suitable and effective thermal management system.

This paper reports: the Thévenin-based equivalent circuit model (Fig. 1) used in the experimental tests (section II), the experimental test bench used for the battery under test (Section III), an overview on the different type of test required for the characterization of the cell (section IV), the results obtained from the extraction parameter procedure (Section V).

## II. BATTERY MODELING

The work starts from a study of the literature models and their performance comparison [13], [14]. Thévenin-based equivalent circuit models are made of a voltage source with a resistance in series and one or more resistance-capacitance parallel blocks. Accuracy and computational efforts of the models depend on the number of RC (Resistance-Capacitance) blocks, higher RC pairs higher the accuracy and the computation time. To account for both fast and slow electrochemical processes of the battery, a second-order Thévenin-based model is preferred concerning the model with only a single RC block. Therefore, the 2nd order or double polarization model represented in Fig. 1 is taken as reference in this paper because it represents a good compromise between accuracy and computational efforts. The battery Open Circuit Voltage (OCV) – e.g. voltage of the battery in a thermochemical equilibrium condition- is represented by a voltage source, whereas the resistance  $R_0$  is used to represent the internal resistance of the cell. Li-ion batteries have high non-linear and non-stationary behavior caused by two different dynamic processes: the activation polarization and the concentration polarization. The first and the second RC block are used to account for these phenomena, respectively. The former overpotential, known as charge transfer polarization, represents the activation energy required to make the electrochemical reactions occur and it's modelled by the first RC pair. The latter or mass-transport overpotential represents the voltage drop due to the concentration gradient inside the battery and it's considered by the second RC block. All the previous parameters are dependent on temperature, SOC, current, thus a high-level accuracy model and a great number of tests are required for the complete electrical and thermal characterization of the battery [19].

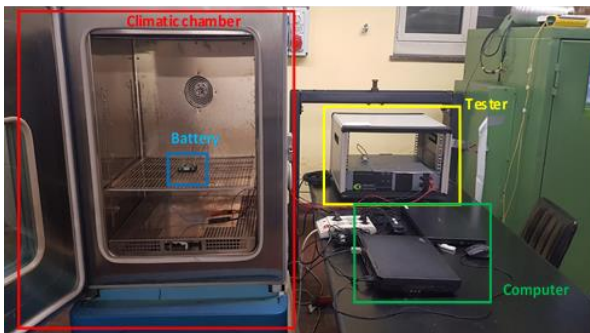


Fig. 2 Laboratory test bench

TABLE I. LG BATTERY CHARACTERISTICS

Property	Value
Nominal capacity	3.0 Ah
Nominal voltage	3.6 V
Max. voltage	4.2 V
Min. voltage	2.5 V
Max. discharge current	20 A
Max. charge current	4 A
Operating temperature	-20 °C to +75 °C
Cycle life	300 cycles

### III. EXPERIMENTAL SETUP

The characterization tests are performed on an LG INR18650HG2 which is a Li-NMC cylindrical cell whose technical specifications are reported in Table 1. Cells under test are placed inside an Angelantoni Challenge 250 climatic chamber and they are linked to MMaterials MM540 battery cell tester through power and signal wires. Figure 2 provides the experimental test bench used for the test. The tester can provide 10 V and 10 A, thus up to 3C discharge tests are available. The software EnergyScope is used to set different types of current or voltage profiles to charge/discharge the battery cell connected to the MMaterials MM540 tester, while the software Winkratos is used to set thermal cycles in terms of temperature and humidity.

The operative temperature range of the climatic chamber is from -40 to +180 °C, thus it's suitable to test the cell in its admissible safety temperature range. The tests have been repeated on five cells of the same stock to get enough statistical value of the results. The data shown in the next paragraph are the weighted average of the five cells results.

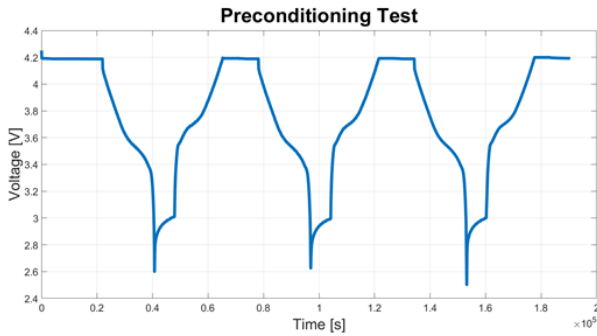


Fig. 3 Voltage profile preconditioning test

### IV. CHARACTERIZATION PROCEDURE

The complete characterization of the cell is made up of different steps and its aim is to evaluate the parameters of the equivalent circuit model presented in Section II. The first type of test consists of the preconditioning of the cells in order to eliminate all the previous hysteresis phenomena caused by different storage conditions, starting from a fully charged cell (Fig. 3). It's made up of a discharge current at C/5 (i.e. 0.6 A), a 6 hours rest period and a charge current at C/5. This cycle is repeated three times, thereafter all the cells are considered to be equal to each other. The second step is to determine the capacity of the cell under test. This parameter gives information about the energy of the battery, thus the amount of charge that the cell supplies or requires during the discharge and charge phase, respectively. Although the manufacturer always provides the value of the nominal capacity of the cell, it's important to carry out this experimental test to obtain a realistic value to be used in the Coulomb counter algorithm for SOC estimation:

$$\text{SOC}(t) = \text{SOC}(0) - 100 \frac{\int_0^t I(t) dt}{C_{3600}} \quad (1)$$

The capacity test consists of a full discharge of the battery from the upper voltage threshold (i.e. 4.2 V) to the lower voltage threshold (i.e. 2.5 V) through the application of a Constant Current (CC). The results of the test are affected by the value of the applied discharge current according to Peukert's law:

$$C_{1C} = I^k \quad (2)$$

Where:  $C_{1C}$  is the capacity of the battery when it is discharged with a current equal to its nominal capacity,  $I$  is the current,  $t$  is the discharging time and  $k$  is the Peukert's coefficient. The current dependency on cell capacity is out of the scope of this paper, thus the value obtained from the 1C test will be taken as a reference for the next test.

The proposed model is the basis for more accurate SOC estimation [20]. This model does not present this kind of SOC calculator to keep the computational effort low.

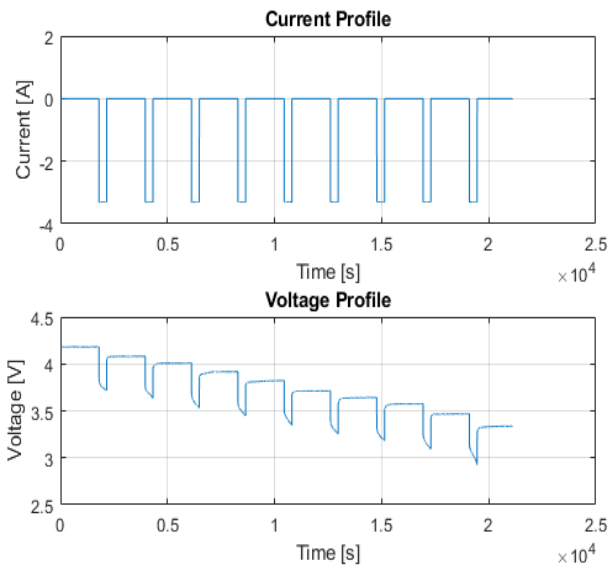


Fig. 4 Voltage and current profiles of the dynamic test

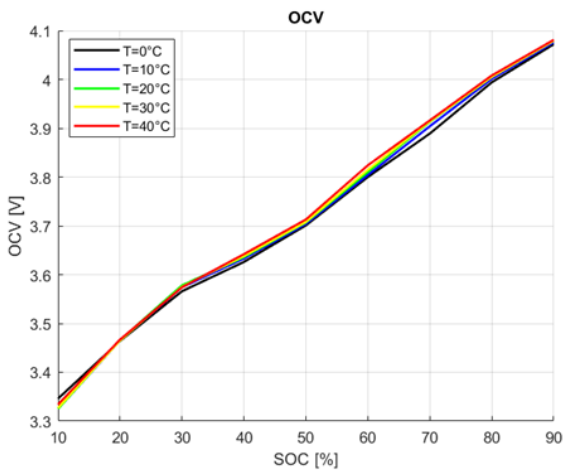


Fig. 5 OCV vs. SOC at different temperatures

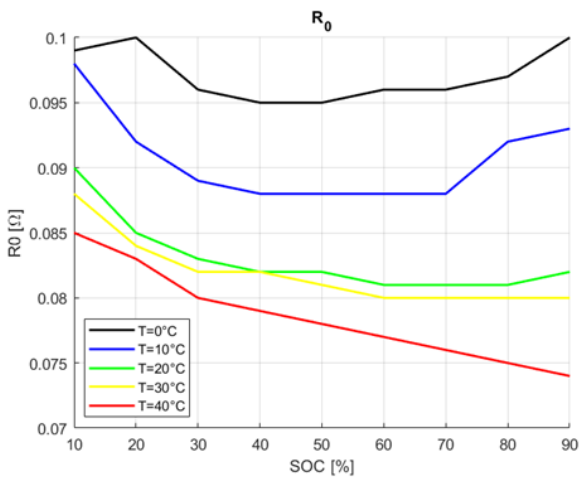


Fig. 5 R0 vs. SOC at different temperatures

The most important test is the Hybrid Pulse Power Characterization (HPPC) which provides the voltage response of the cell when it's stressed by a dynamic current profile. It consists of a series of current pulses

and rest times across the whole battery SOC range and during which the battery voltage is measured. The fully charged battery (4.2 V) is discharged with a series of 1C current pulses each one followed by a rest period of 30 minutes until the cell lower voltage threshold (2.5 V) is reached. A discharge of 10% of the battery capacity occurs during each current pulse. The equivalent circuit parameters are calculated during each rest period in order to evaluate their dependency from SOC. The current and voltage waveforms are shown in Fig. 4.

The cells under test are placed inside a climatic chamber in order to keep the temperature of the cell constant during the whole test.

The thermal profile of the climatic chamber is made up of three steps:

- A 15 minutes ramp to reach the test temperature set point.
- A 6 hours constant temperature section to perform the HPPC test.
- A 15 minutes ramp to come back to the ambient temperature.

Finally, the HPPC test is repeated for temperature equal to 0, 10, 20, 30 and 40 °C in order to evaluate how the parameters of the Thévenin based model are a function of both battery temperature and SOC. The results are used to create a two-dimensional lookup table for each parameter of the EEC model, suitable for the accurate estimation of the heat generation rate inside the cell during its discharging phase, through the equation:

$$Q = I(OCV - V) - IT \frac{\partial OCV}{\partial T} \quad (3)$$

Where:  $I$  is the discharge current,  $V$  is the voltage of the cell,  $T$  is the temperature of the cell. In particular, the current applied is a known value, OCV and its derivative with temperature are extracted from the lookup table, the cell voltage is calculated solving the 2<sup>nd</sup> Kirchhoff law applied to the EEC, and  $T$  is evaluated through a model which will be dealt in a next paper. In equation (3) the first term represents the irreversible heat due to the Joule effect, whereas the second term represents the entropic reversible heat linked to the electrochemical reactions.

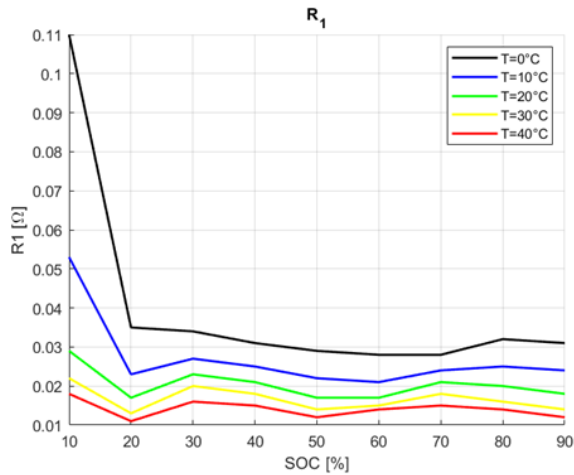


Fig. 7 R1 vs. SOC at different temperatures

## V. PARAMETERS EXTRACTION

The parameters of the EEC model are extracted from the analysis of the voltage response of the battery during the rest period when SOC remains constant. The OCV is equal to the last measured voltage of the relaxation period, while the value of R0 is calculated as the ratio between the impulsive voltage variation at the end of the pulse and the discharge current. The remaining parameters are extracted using a curve-fitting procedure carried out using a properly made program developed in MATLAB environment. A

complete and more accurate description of the parameter extraction procedure is presented in [21]. The SOC and temperature dependence of the EEC parameters are shown from Figure 5 to Figure 10.

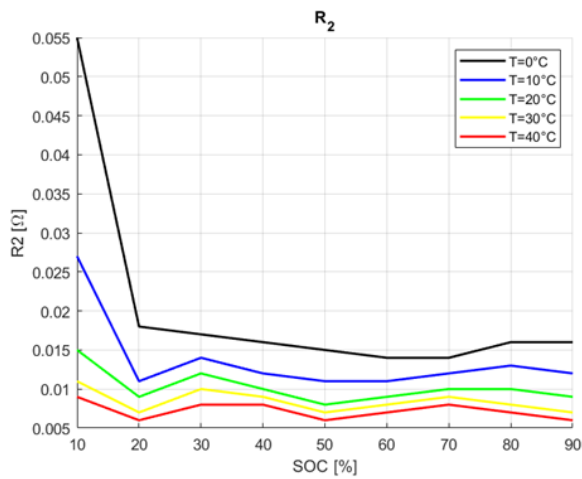


Fig. 8  $R_2$  vs. SOC at different temperatures

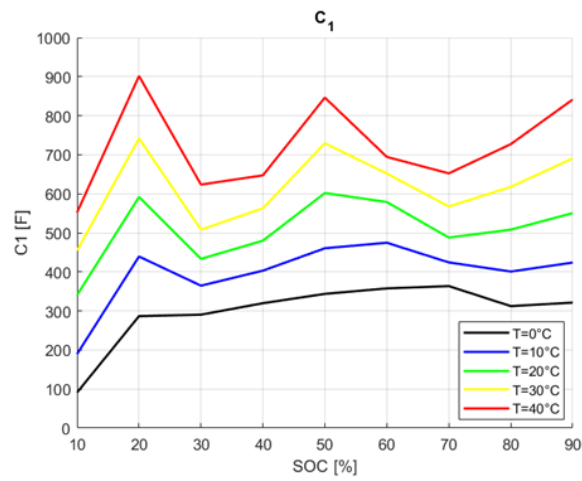


Fig. 9  $C_1$  vs. SOC at different temperatures

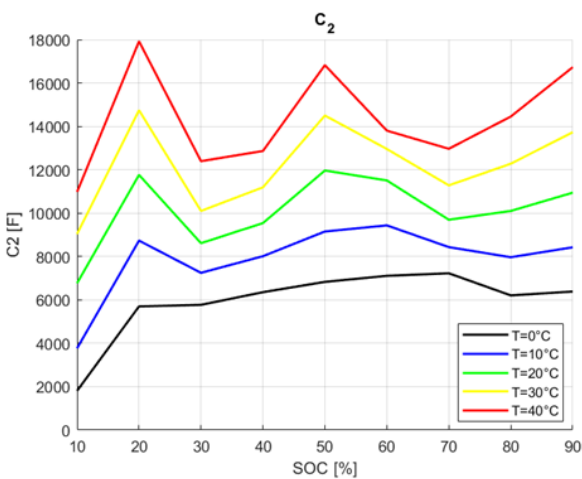


Fig. 10  $C_2$  vs. SOC at different temperatures

The OCV decreases with SOC since the battery is discharging. For the value of SOC higher than 10% the OCV increases with temperature, the opposite trend occurs for SOC lower than 10%. Therefore, the cut-off voltage is inversely dependent on temperature determining a reduction of the capacity of the cell. On

the other hand, the resistances  $R_0$ ,  $R_1$ , and  $R_2$  decreases with temperature, whereas the capacitances  $C_1$  and  $C_2$  increases with temperature. Resistance and capacitance trends are explained by the fact that higher temperatures promote ion diffusion and reaction rate. Moreover, the evolution of the derivative of the open-circuit voltage with respect to the temperature can be obtained from the OCV lookup table and can be used in equation (3) for the calculation of the cell heat source term (Fig. 11). Finally, in **Errore. L'origine riferimento non è stata trovata.** the evolution of the heat generation rate inside the cell is evaluated during the 1C discharge phase.

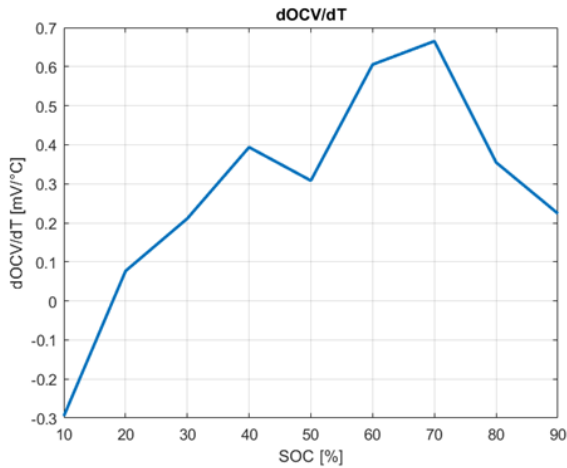


Fig. 11 dOCV/dT vs. SOC

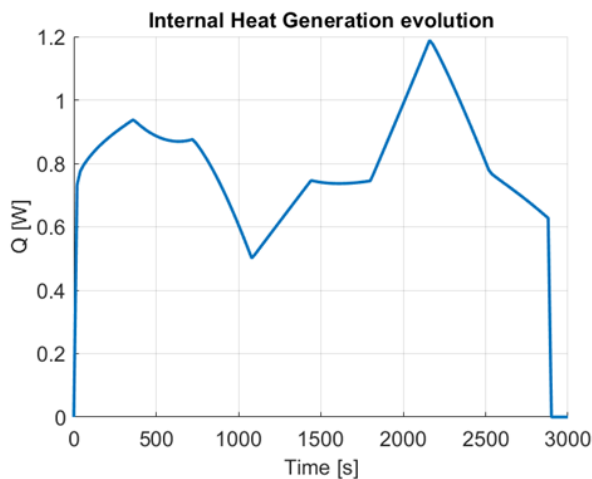


Fig. 12 Heat generation rate during 1C discharge

## VI. CONCLUSION

In this paper, a double polarization Thévenin equivalent circuit model was used to accurately simulate the dynamic behavior of Li-ion batteries in electric control vehicle applications.

To estimate the parameters of the model a hybrid pulse power characterization test was used. The test was performed inside a climatic chamber to evaluate the dependence of the extracted parameters from both temperature and state of charge. Analyzing the results of the test it's possible to make the following considerations:

- The open-circuit voltage decreases with SOC and increases with temperature.
- The resistances  $R_0$ ,  $R_1$ , and  $R_2$  increase when temperature decreases. Thus, lower the operative temperature higher the heat generation rate inside the cell according to the Joule heating effect.
- The capacitances  $C_1$  and  $C_2$  increase with temperature

From the electrical characterization of the cell, it's possible to conclude that the optimal temperature range of the battery is 20-40°C. In this temperature window, enhancement of cell performances occurs

thanks to a lower value of the internal battery resistance which determines an increase of the electrochemical reaction rates. Since no tests have been done to evaluate the battery cell performance dependency on current rate and current direction, this will be the object of future work from the authors, to extend the model validity to a broader set of operating conditions. Furthermore, a more elaborate SOC estimator, based on Kalman Filter, will be implemented in the proposed model to be more accurate. Moreover, the presented results will be the input of a thermal model able to determine temperature evolution inside the battery during a complete discharging profile. These results will be also the basis for the design of an effective thermal management system for the whole battery pack cooling.

#### ACKNOWLEDGMENT

The authors want to acknowledge the Innovative Electric and Hybrid Vehicle IEHV Research group (Politecnico di Torino- DIMEAS) for providing instrumentation and facilities.

#### REFERENCES

- [1] M. Varini, P. E. Campana, e G. Lindbergh, «A semi-empirical, electrochemistry-based model for Li-ion battery performance prediction over lifetime», *J. Energy Storage*, vol. 25, pag. 100819, ott. 2019, doi: 10.1016/j.est.2019.100819.
- [2] G. Zubi, R. Dufo-López, M. Carvalho, e G. Pasaoglu, «The lithium-ion battery: State of the art and future perspectives», *Renew. Sustain. Energy Rev.*, vol. 89, pagg. 292–308, giu. 2018, doi: 10.1016/j.rser.2018.03.002.
- [3] M. A. Hannan, Md. M. Hoque, A. Hussain, Y. Yusof, e P. J. Ker, «State-of-the-Art and Energy Management System of Lithium-Ion Batteries in Electric Vehicle Applications: Issues and Recommendations», *IEEE Access*, vol. 6, pagg. 19362–19378, 2018, doi: 10.1109/ACCESS.2018.2817655.
- [4] A. Ferraris et al., «Nafion® Tubing Humidification System for Polymer Electrolyte Membrane Fuel Cells», *Energies*, vol. 12, n. 9, pag. 1773, mag. 2019, doi: 10.3390/en12091773.
- [5] M. Carello, V. De Vita e A. Ferraris, «Method for Increasing the Humidity in Polymer Electrolyte Membrane Fuel Cell», *Fuel Cells*, vol. 16, n. 2, pagg. 157–164, 2016, doi: 10.1002/face.201500110.
- [6] Y. Ji, Y. Zhang, e C.-Y. Wang, «Li-Ion Cell Operation at Low Temperatures», *J. Electrochem. Soc.*, vol. 160, n. 4, pagg. A636–A649, 2013, doi: 10.1149/2.047304jes.
- [7] D. Chen, J. Jiang, G.-H. Kim, C. Yang, e A. Pesaran, «Comparison of different cooling methods for lithium ion battery cells», *Appl. Therm. Eng.*, vol. 94, pagg. 846–854, feb. 2016, doi: 10.1016/j.applthermaleng.2015.10.015.
- [8] H.-C. (Alex) Shiao, D. Chua, H. Lin, S. Slane, e M. Salomon, «Low temperature electrolytes for Li-ion PVDF cells», *J. Power Sources*, vol. 87, n. 1–2, pagg. 167–173, apr. 2000, doi: 10.1016/S0378-7753(99)00470-X.
- [9] S. S. Zhang, K. Xu, e T. R. Jow, «Low temperature performance of graphite electrode in Li-ion cells», *Electrochimica Acta*, vol. 48, n. 3, pagg. 241–246, dic. 2002, doi: 10.1016/S0013-4686(02)00620-5.
- [10] S. Ma et al., «Temperature effect and thermal impact in lithium-ion batteries: A review», *Prog. Nat. Sci. Mater. Int.*, vol. 28, n. 6, pagg. 653–666, dic. 2018, doi: 10.1016/j.pnsc.2018.11.002.
- [11] Z. Wang, J. Ma, e L. Zhang, «Finite Element Thermal Model and Simulation for a Cylindrical Li-Ion Battery», *IEEE Access*, vol. 5, pagg. 15372–15379, 2017, doi: 10.1109/ACCESS.2017.2723436.
- [12] A. De Vita, A. Maheshwari, M. Destro, M. Santarelli, e M. Carello, «Transient thermal analysis of a lithium-ion battery pack comparing different cooling solutions for automotive applications», *Appl. Energy*, vol. 206, pagg. 101–112, nov. 2017, doi: 10.1016/j.apenergy.2017.08.184.
- [13] [U. Krewer, F. Röder, E. Harinath, R. D. Braatz, B. Bedürftig, e R. Findeisen, «Review—Dynamic Models of Li-Ion Batteries for Diagnosis and Operation: A Review and Perspective», *J. Electrochem. Soc.*, vol. 165, n. 16, pagg. A3656–A3673, 2018, doi: 10.1149/2.1061814jes.
- [14] F. Saidani, F. X. Hutter, R.-G. Scurtu, W. Braunwarth, e J. N. Burghartz, «Lithium-ion battery models: a comparative study and a model-based powerline communication», *Adv. Radio Sci.*, vol. 15, pagg. 83–91, set. 2017, doi: 10.5194/ars-15-83-2017.
- [15] S. Scavuzzo et al., «Simplified Modeling and Characterization of the Internal Impedance of Lithium-Ion Batteries for Automotive Applications», in *2019 AEIT International Conference of Electrical and Electronic Technologies for Automotive (AEIT AUTOMOTIVE)*, Torino, Italy, lug. 2019, pagg. 1–6, doi: 10.23919/EETA.2019.8804553.
- [16] E. Locorotondo et al., «Modeling and simulation of Constant Phase Element for battery Electrochemical Impedance Spectroscopy», set. 2019.
- [17] E. Locorotondo et al., «Electrochemical Impedance Spectroscopy of Li-Ion battery on-board the Electric Vehicles based on Fast nonparametric identification method», in *2019 IEEE International Conference on Environment and Electrical Engineering and 2019 IEEE Industrial and Commercial Power Systems Europe (EEEIC / I&CPS Europe)*, Genova, Italy, giu. 2019, pagg. 1–6, doi: 10.1109/EEEIC.2019.8783625.
- [18] S. Buller, M. Thele, E. Karden, e R. W. De Doncker, «Impedance-based non-linear dynamic battery modeling for automotive applications», *J. Power Sources*, vol. 113, n. 2, pagg. 422–430, gen. 2003, doi: 10.1016/S0378-7753(02)00558-X.
- [19] D. Cittanti, A. Ferraris, A. Airale, S. Fiorot, S. Scavuzzo, e M. Carello, «Modeling Li-ion batteries for automotive application: A trade-off between accuracy and complexity», in *2017 International*

Conference of Electrical and Electronic Technologies for Automotive, giu. 2017, pagg. 1–8, doi: 10.23919/EETA.2017.7993213.

- [20] C. Zhang, J. Jiang, W. Zhang, e S. M. Sharkh, «Estimation of State of Charge of Lithium-Ion Batteries Used in HEV Using Robust Extended Kalman Filtering», *Energies*, vol. 5, n. 4, pagg. 1098–1115, apr. 2012, doi: 10.3390/en5041098.
- [21] A. Hentunen, T. Lehmuspelto, e J. Suomela, «Time-Domain Parameter Extraction Method for Thevenin-Equivalent Circuit Battery Models», *IEEE Trans. Energy Convers.*, vol. 29, n. 3, pagg. 558–566, set. 2014, doi: 10.1109/TEC.2014.2318205.